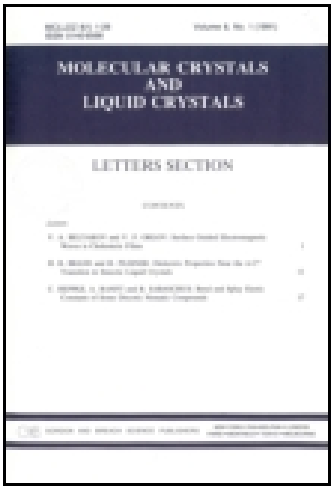

Molecular Crystals and Liquid Crystals
Publication details, including instructions for authors and subscription information:
http://www.tandfonline.com/loi/gmcl20

Enhanced Light Harvesting and Electron Lifetime of Front Side-illuminated CdSe Quantum Dot-assembled TiO_2 Nanotube Arrays for Quantum Dot-sensitized Solar Cells

Sung Woo Jung[a], Soo-Yong Lee[a], Min-Ah Park[a], Jae-Hong Kim[a], Soon-Hyung Kang[b], Hyunsoo Kim[c], Chel-Jong Choi[c] & Kwang-Soon Ahn[a]

[a] School of Chemical Engineering, Yeungnam University, Gyeongsan, S. Korea

[b] Department of Chemistry Education, Chonnam National University, Gwangju, S. Korea

[c] School of Semiconductor and Chemical Engineering, Chonbuk National University, Jeonju, S. Korea

Published online: 17 Nov 2014.

To cite this article: Sung Woo Jung, Soo-Yong Lee, Min-Ah Park, Jae-Hong Kim, Soon-Hyung Kang, Hyunsoo Kim, Chel-Jong Choi & Kwang-Soon Ahn (2014) Enhanced Light Harvesting and Electron Lifetime of Front Side-illuminated CdSe Quantum Dot-assembled TiO_2 Nanotube Arrays for Quantum Dot-sensitized Solar Cells, Molecular Crystals and Liquid Crystals, 598:1, 144-153, DOI: 10.1080/15421406.2014.933386

To link to this article: http://dx.doi.org/10.1080/15421406.2014.933386

Mol. Cryst. Liq. Cryst., Vol. 598: pp. 144–153, 2014

ISSN: 1542-1406 print/1563-5287 online
DOI: 10.1080/15421406.2014.933386

Taylor & Francis
Taylor & Francis Group

Enhanced Light Harvesting and Electron Lifetime of Front Side-illuminated CdSe Quantum Dot-assembled TiO_2 Nanotube Arrays for Quantum Dot-sensitized Solar Cells

SUNG WOO JUNG,[1] SOO-YONG LEE,[1] MIN-AH PARK,[1] JAE-HONG KIM,[1] SOON-HYUNG KANG,[2] HYUNSOO KIM,[3] CHEL-JONG CHOI,[3,*] AND KWANG-SOON AHN[1,*]

[1]School of Chemical Engineering, Yeungnam University, Gyeongsan, S. Korea
[2]Department of Chemistry Education, Chonnam National University, Gwangju, S. Korea
[3]School of Semiconductor and Chemical Engineering, Chonbuk National University, Jeonju, S. Korea

CdSe quantum dots (QDs)-assembled, free-standing TiO_2 nanotube arrays (TNTs) are transferred to transparent fluorine-doped tin oxides (FTOs) using a sol-gel process. The TNTs on the FTO (FTO/TNT) not only provide an efficient 1-dimensional electron pathway with few recombination centers, but also allow front side illumination through the transparent FTO, providing a significantly enhanced electron lifetime and light harvesting compared to conventional TNTs on Ti foil and TiO_2 nanoparticles-based mesoporous films on the FTO. These effects help improve significantly the short circuit current and open-circuit voltage of quantum dot-sensitized solar cells (QD-SSCs).

Keywords quantum dot-sensitized solar cell; nanotube array; front side illumination; electron lifetime; light harvesting

1. Introduction

Mesoporous TiO_2-based dye-sensitized solar cells (DSSCs) are potential low-cost alternatives to commercial Si-based solar cells [1–4]. These cells consist of a dye-sensitized mesoporous TiO_2 layer and a Pt counter electrode with an electrolyte containing a redox couple (I^-/I_3^-) between them. The use of a ruthenium complex photo-sensitizer has resulted in an overall energy-conversion efficiency of 12% [5].

Both Prof. K.-S. Ahn and C.-J. Choi contibuted equally to this work as the corresponding authors.

*Address correspondence to K.-S. Ahn, School of Chemical Engineering, Yeungnam University, Gyeongsan 712-749, S. Korea. (Tel.)+82-53-810-2524, (Fax)+82-53-810-4631, E-mail: kstheory@ynu.ac.kr; C.-J. Choi, School of Semiconductor and Chemical Engineering, Chonbuk National University, Jeonju 561-756, S. Korea. (Tel.)+82-63-270-3365, (Fax)+82-63-270-3972, E-mail: cjchoi@jbnu.ac.kr

Color versions of one or more of the figures in the article can be found online at www.tandfonline.com/gmcl.

Semiconducting quantum dots (QDs), such as CdS, CdSe, PbS and InP have been tested as photo-sensitizers for DSSCs [6–14] because their optical band gaps can be adjusted easily through quantum confinement effects by varying their size [6,7,12–14]. In addition, these materials are robust, inorganic materials with higher extinction coefficients than conventional dyes due to the existence of multiple levels [6–9]. On the other hand, despite the advantages of QDs, quantum dot-sensitized solar cells (QD-SSCs) still have low energy conversion [6,9].

Conventional mesoporous TiO_2 films composed of nanoparticles smaller than 30 nm do not develop a depletion layer at the interface between the TiO_2 and electrolyte. This causes large back electron transfer from the conduction band of TiO_2 to the electrolyte due to trap-limited diffusion [15,16]. The suppression of back electron transfer has been attempted using 1-dimensional (1-D) nanostructures (nanotubes, nanorods, etc.) with faster electron transport [17–22]. TiO_2 nanotube arrays (TNTs) have been fabricated by electrochemically anodizing Ti metallic foils in a F^- ion-containing solution [17–20]. In contrast, QD-SSCs employing TNTs on a Ti foil (Ti foil/TNT) have a critical limitation caused by the opacity of the Ti metallic substrates, which require back side illumination when used as photoanodes in solar cells [4,23]. At back side illumination, the counter electrodes (CEs) should be as transparent as possible otherwise they will reflect light. Furthermore, with back side illumination, the polysulfide electrolytes absorb photons, which reduce the level of light harvesting significantly [12,23]. Recently, to overcome this issue, front side-illuminated TNTs have been realized by transferring the free-standing TNTs to the transparent fluorine-doped tin oxides (FTOs) [23–26]. Most front side-illuminated FTO/TNTs have been applied to the DSSCs [23–26], whereas there have been few studies on QD-SSCs [27].

In this article, free-standing crystallized TNTs were prepared by two-step anodization followed by a selective etching process in a H_2O_2 solution, which were then transferred to the transparent FTO substrates by a sol-gel process. For comparison, the conventional TNTs (TNT on the Ti metallic foil) and TiO_2 nanoparticles (TNP)-based mesoporous film on the FTO (FTO/TNP) were prepared. The QD-SSC with the front side-illuminated FTO/TNT/CdSe showed significantly enhanced overall energy conversion efficiency, compared to those with the back side-illuminated Ti foil/TNT/CdSe and front side-illuminated FTO/TNP/CdSe. These results were studied systematically in terms of the electron lifetime, light harvesting, recombination rate, optical band gap and crystallographic structure.

2. Experimental

2.1. Preparation of the TiO_2 Films (Ti foil/TNT, FTO/TNT, and FTO/TNP)

2.1.1. Preparation of the Ti foil/TNT. Ti foil (Goodfellow, 0.1 mm thickness, 99.6% purity) was used for the anodic growth of TiO_2 nanotubes. The foil was ground roughly, cleaned by sonication in acetone and ethanol, and then rinsed in de-ionized water (DI). Electrochemical anodization was carried out at 60 V for 3 h with 3 cm separation between the working (Ti foil) and counter electrode (Pt mesh) [17–20]. The electrolyte consisted of 0.25 wt.% NH_4F in ethylene glycol containing a 1 M (mol/L) water. The 18 μm-thick, amorphous TiO_2 nanotubes (Ti foil/a-TNT) were sonicated in ethanol for 5 min to remove any remnants from the surfaces and dried in an air stream. They were then annealed at 450°C for 4 h in air for crystalline TiO_2 nanotubes (Ti foil/c-TNT).

2.1.2. Preparation of the FTO/TNT. The Ti foil/c-TNTs were anodized again in the same stock electrolyte for 1 h with a potential of 12 V to form an amorphous TiO_2 layer between

the crystallized TiO_2 nanotube arrays and Ti foil [22]. The two-step anodized samples were then immersed into a 5% H_2O_2 solution for 2 h to selectively dissolve the amorphous TiO_2, resulting in free-standing c-TNTs. The freestanding c-TNTs were then adhered to the FTO substrates with one drop of the Ti precursor-containing sol (0.1 M titanium isopropoxide (TTIP) in isopropanol and 5 wt.% ethyl cellulose). The films were finally annealed at 450°C for 4 h at a heating rate of 1°C min^{-1} for the interconnection between the FTO and TNTs with the formation of a thin TiO_2 interlayer.

2.1.3. Preparation of the FTO/TNP. Nanoparticle-based mesoporous TiO_2 films were prepared by doctor-blading a TiO_2 paste (Ti-Nanoxide T/SP, Solaronix SA) onto the FTO substrates, followed by sintering at 450°C for 4 h in air. The films were deposited to a similar film thickness (18 μm).

2.2. Deposition of CdSe Quantum Dots on the TiO_2 Samples

CdSe QDs were assembled on the TiO_2 films by successive ionic layer adsorption and reaction (SILAR) [28,29]. For the synthesis of CdSe QDs, ethanol was used to dissolve 30 mM $Cd(NO_3)_2$ and sodium selenide in a glove box, respectively. Sodium selenide was made by 30 mM SeO_2 and 60 mM $NaBH_4$. The SILAR process involved immersing the TiO_2 films in a $Cd(NO_3)_2$ solution for 1 min, rinsing it with ethanol, followed by further immersion in a sodium selenide solution for 1 min, and rinsing with ethanol. Each two-step immersions constituted a single SILAR cycle. The SILAR procedure was carried out on the TiO_2 samples for eight cycles.

2.3. Cell Fabrication

Semitransparent Pt counter electrodes (CEs) were prepared by doctor-blading a Pt nanocluster-containing Pt paste (PT-1, Dyesol. Ltd.) onto FTO substrates followed by calcination at 450°C for 30 min in air. The TiO_2 samples and semitransparent Pt counter electrodes (CEs) were sandwiched using 60 μm-thick sealing material. A polysulfide electrolyte (0.5 M Na_2S, 2 M S, and 0.2 M KCl) prepared using water/methanol (3:7 by volume) was used. All TiO_2 samples had similar active areas of QD-sensitized photoanodes of 0.16 cm^2.

2.4. Characterization

QD-SSCs with the FTO/TNT/CdSe and FTO/TNP/CdSe were illuminated from the front side, whereas QD-SSCs with the Ti foil/TNT/CdSe were illuminated from the back side, i.e. from the semitransparent Pt counter electrode because of the opacity of the Ti metallic foil. Their photovoltaic current-voltage characteristics were measured using the solar simulator (PEC-L11, Peccell Ltd.) under 1 Sun illumination (100 $mWcm^{-2}$, AM 1.5), which was verified using an AIST-calibrated Si-solar cell. For the open-circuit voltage decay (OCVD) measurements, the cells were illuminated to a steady voltage and the decay in the open-circuit voltage was then measured after the illumination was cut off with a shutter. The incident photon-to-current conversion efficiency (IPCE) was measured using an action spectrum measurement setup (PEC-S20, Peccell Ltd.) in a DC mode without the white bias. The QD sizes on TiO_2 were measured by diffuse reflectance absorption spectroscopy (Cary5000, Agilent Tech. Co.). The morphology and crystallographic structures of the TiO_2 samples were characterized by scanning electron microscopy (SEM, Hitachi FE-SEM S4800) and X-ray diffraction (XRD, PANalytical), respectively.

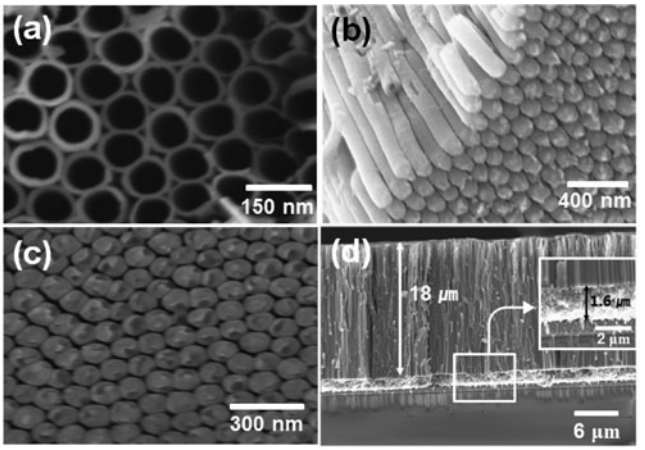

Figure 1. SEM images; (a) top view, (b) cross-sectional view, and (c) the bottom view of the free-standing crystallized TNT detached from the Ti foil. (d) cross-sectional view of the FTO/TNT. The inset figure in (d) shows the TiO_2 nanoporous interlayer.

3. Results and Discussion

Figure 1 shows FE-SEM images of (a) top view, (b) cross-sectional view, and (c) the bottom view of the free-standing crystallized TNT. The top-view SEM image shows that the TiO_2 nanotube arrays comprised of separated nanotubes with a mean internal diameter and wall thickness of 80 ± 3 nm and 13 nm, respectively. The free-standing TNT arrays remained compact and no destruction was observed after being peeled off from the Ti metallic foil. The bottom view showed that the TNT arrays were well preserved. The free-standing TNT was transferred successfully onto the FTO substrate using a sol-gel process, as shown in the Fig. 2(d). A 1.6 μm-thick TiO_2 nanoporous thin layer was formed as an interlayer, which connected the TNT arrays with the FTO substrate.

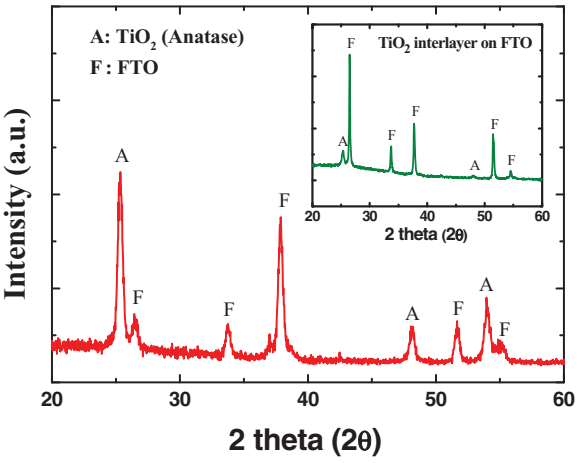

Figure 2. (Color online) X-ray diffraction pattern of the FTO/TNT film. The inset shows the XRD pattern of TiO_2 nanoporous interlayer on the FTO.

Figure 2 shows the XRD pattern of the FTO/TNT film, indicating the anatase phase. To examine the crystallographic structure of the TiO_2 thin interlayer formed between the FTO and TNT, the TTIP precursor was dip-coated on the FTO and annealed at 450°C in air without transferring the TiO_2 nanotube arrays. The XRD pattern clearly showed that the TiO_2 interlayer prepared from the sol-gel process had the same anatase phase as the TNTs (Inset in Fig. 2). In addition, from the Debye-Sherrer equation, the TiO_2 interlayer had a nanoporous structure consisting of nanoparticles with a mean size of 20 nm.

CdSe QDs were assembled on all of the TiO_2 samples (FTO/TNT, Ti foil/TNT, and FTO/TNP) using the same SILAR process. The Brus equation was used to estimate the mean diameters of the CdSe QDs on the TiO_2 samples [8,30]:

$$E_{QD} = E_g + \frac{h^2}{8r^2}\left[\frac{1}{m_e^*} + \frac{1}{m_h^*}\right] - \frac{1.8e^2}{4\pi\varepsilon\varepsilon_0 r} \tag{1}$$

where E_{QD} and E_g are the lowest excitation energy of the QDs and the band gap of bulk CdSe, respectively. r is the radius of the CdSe QDs. $m_e{}^*$ and $m_h{}^*$ are the effective masses of electrons and holes in CdSe, respectively, ε_0 is the vacuum permittivity, and ε is the relative permittivity of CdSe. From the diffuse reflectance absorbance curves (not shown here), the CdSe QDs were estimated to be deposited with similar sizes on all of the TiO_2 films (diameter: 6.3 nm, 6.0 nm and 6.3 nm for the FTO/TNT, Ti foil/TNT, and FTO/TNP, respectively). The QDs were assembled by the SILAR process. The SILAR has the advantages of *in situ* deposition whereas it has the disadvantages of making it difficult to estimate how much the QDs were covered. In this experiment, the QDs assembled on the TNT and TNP exhibited almost similar QDs' average sizes in the range from 6.0 to 6.3 nm, inferring that the QDs were covered on the all of the TiO2 films similarly.

The electron lifetimes were estimated from open circuit voltage decay (OCVD) measurements [4,31]. Figure 3(a) shows the V_{oc} decay curves of the QD-SSCs recorded during relaxation from the illuminated quasi-equilibrium state to darkness. Figure 3(b) presents the electron lifetimes estimated from the V_{oc} decay curves according to the following equation [31]:

$$\tau_e = -\frac{k_B T}{e}\left[\frac{dV_{oc}}{dt}\right]^{-1} \tag{2}$$

where k_BT is the thermal energy, e is the positive elementary charge and dV_{oc}/dt is the derivative of the open circuit voltage transient. The photovoltage decay rate is related directly to the electron lifetime because excess electrons are removed through recombination when the illumination of the QD-SSCs at the open circuit is interrupted. This means that the electron lifetime is dependent on back electron transfer from TiO_2 to the redox couple. The CdSe QD-assembled FTO/TNT (FTO/TNT/CdSe) exhibited a much longer electron lifetime than the CdSe QD-assembled FTO/TNP (FTO/TNP/CdSe). This is because the 1-dimensionally (1-D) nanostructured TNT provides fewer recombination centers than the TNPs with a 3-D network [32,33]. The FTO/TNT/CdSe exhibited a similar electron lifetime to the Ti foil/TNT/CdSe, indicating that the electron lifetime is dominated mainly by the nanostructural properties of TiO_2 itself, regardless of the substrates.

Figure 4(a) shows the photovoltaic current-voltage (I-V) performance of the QD-SSCs under 1 Sun illumination, which are summarized in Table 1. These results were reproducible. Unlike the back side-illuminated QD-SSC with the Ti foil/TNT/CdSe, the QD-SSCs with the FTO/TNT/CdSe exhibited significantly improved cell efficiency compared to that with the FTO/TNP/CdSe. The significantly enhanced cell efficiency of the QD-SSCs with the

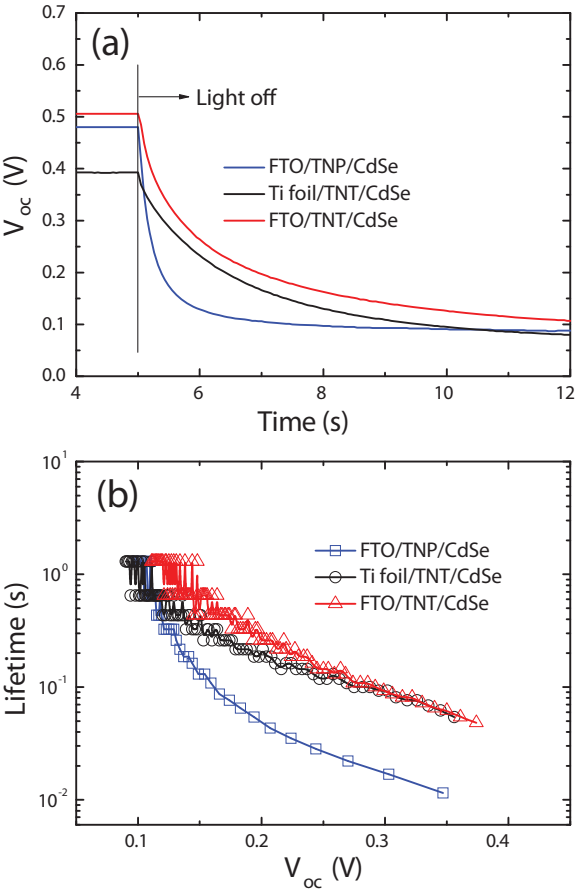

Figure 3. (Color online) (a) V_{oc} decay curves of the QD-SSCs with the FTO/TNT/CdSe, Ti foil/TNT/CdSe and FTO/TNP/CdSe recorded during relaxation from illuminated quasi-equilibrium to darkness. (b) Electron lifetimes estimated from (a).

FTO/TNT/CdSe was due mainly to the significantly enhanced short-circuit current (J_{sc}) and open-circuit voltage (V_{oc}). The J_{sc} was studied in more detail using the incident photon-to-current conversion efficiency (IPCE) curves [Fig. 6(b)]. Unlike the p-n junction Si solar cells, the electron transport in the QD-SSCs is driven by the diffusion mechanism other than the drift mechanism, indicating relatively slow electron transport in the QD-SSCs.

Table 1. Photovoltaic performances of the QD-SSCs

Samples	J_{sc} mAcm^{-2}	V_{oc} V	FF %	η %
QD-SSC with FTO/TNP/CdSe [a]	10.94	0.48	35.32	1.85
QD-SSC with Ti foil/TNT/CdSe [b]	6.85	0.39	35.16	0.94
QD-SSC with FTO/TNT/CdSe [a]	16.02	0.51	29.74	2.43

[a]Illuminated in front side mode, [b]Illuminated in back side mode

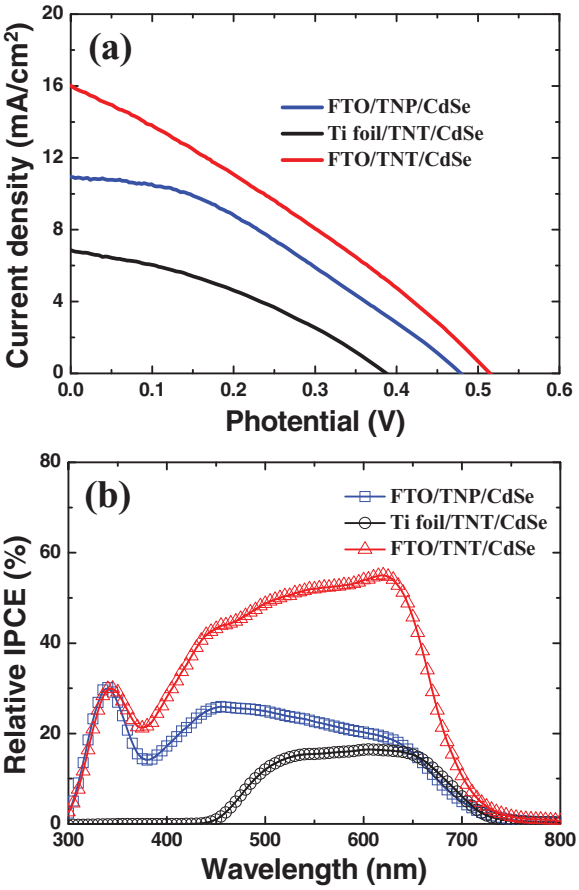

Figure 4. (Color online) (a) Photovoltaic current-voltage curves of the QD-SSCs with the FTO/TNT/CdSe, Ti foil/TNT/CdSe, and FTO/TNP/CdSe measured under 1 Sun illumination. (b) Relative incident photon-to-current conversion efficiencies (IPCEs) of the QD-SSCs.

The IPCE strongly depends on the bias light, which makes it difficult to obtain accurate IPCE spectra of the QD-SSCs. In this experiment, the IPCEs were measured in a DC mode without the white bias, but the IPCEs were measured in the same measurement condition for all the samples, indicating that the IPCEs could be relatively compared and evaluated. IPCE is the product of three factors, light-harvesting efficiency (LHE), charge-injection efficiency (η_{inj}) and charge-collection efficiency (η_{cc}) [34,35]:

$$IPCE = LHE \cdot \eta_{inj} \cdot \eta_{cc} \tag{3}$$

All the QD-SSCs exhibited the same onset wavelength, indicating that the CdSe QDs were assembled with similar sizes on all TiO_2 films, which correspond well to the results in Fig. 4. η_{inj} is determined by the driving force related to the energy difference between the conduction bands of TiO_2 and QDs. [6] The QDs deposited with similar sizes imply a similar energy difference between the conduction bands of TiO_2 and the QDs, indicating a similar η_{inj} for all TiO_2 films examined. The QD-SSCs with the Ti foil/TNT/CdSe were illuminated in back side mode due to the opacity of the Ti foil substrate. The IPCE of

the QD-SSC with the Ti foil/TNT/CdSe was reduced abruptly at below 500 nm. This was attributed mainly to light absorption by the sulfur-containing electrolyte caused by back side illumination. Furthermore, the QD-SSCs with Ti foil/TNT/CdSe showed a lower IPCE at wavelengths above 500 nm than that with the FTO/TNP/CdSe, despite its much longer electron lifetime, which was attributed to the light reflection from the semitransparent Pt counter electrode (CE). This means that the LHE is reduced significantly due to the light absorption of the electrolyte and the light reflection of the Pt CE, which is responsible for the low cell efficiency of the QD-SSCs with the Ti foil/TNT/CdSe. On the other hand, the QD-SSC with FTO/TNT/CdSe allows front side illumination, which does not have any light absorption loss caused by the electrolyte and Pt CE. In addition, the TNTs provided a longer electron lifetime than the TNPs, as shown in Fig. 3. These beneficial effects enhanced the IPCE significantly, which contributed to a significantly higher J_{sc}.

The significantly improved cell efficiency of the QD-SSC with the FTO/TNT/CdSe was also affected by the increased V_{oc}. The V_{oc} is closely related to charge injection and the recombination rate [36,37];

$$V_{oc} = \left(\frac{k_B T}{e}\right) \mathrm{In} \left(\frac{J_{inj}}{n_{cb} k_{et} \left[S_X^{2-}\right]}\right) \tag{4}$$

where J_{inj} is the current due to the electrons from the excited QD and can be defined as the sum of the short-circuit current and dark current. n_{cb} and k_{et} are the concentration of electrons at the TiO_2 surface and the rate constant for the reduction of polysulfide (S_x^{2-}), respectively. The QD-SSCs with the Ti foil/TNT/CdSe exhibited a lower V_{oc} than that with the FTO/TNP/CdSe, despite the much longer electron lifetime. This was attributed to the J_{inj} being reduced significantly by the light absorption loss in back side illumination mode. In contrast, the QD-SSCs with FTO/TNT/CdSe exhibited a significantly higher V_{oc} compared to that with the FTO/TNP/CdSe. The QD-SSC with the FTO/TNT/CdSe does not have any light absorption loss by the electrolyte and Pt CE. Furthermore, the nanotubular structure of the TNTs led to a significant increase in electron lifetime, indicating that back electron transfer (or recombination) from the TiO_2 to the electrolyte was suppressed. Therefore, the significantly increased V_{oc} of the QD-SSC with the FTO/TNT/CdSe was due mainly to the hindered recombination rate (reduced k_{et}).

4. Conclusions

Free-standing c-TNTs were transferred to a transparent FTO substrate using a sol-gel process with the TTIP precursor. The CdSe QDs with similar sizes were assembled not only on the FTO/TNT but also on the Ti foil/TNT and FTO/TNP prepared for comparison. The QD-SSCs with the Ti foil/TNT/CdSe require back side illumination, causing light absorption and reflection by the electrolyte and semitransparent Pt counter electrode. On the other hand, the QD-SSCs with the FTO/TNT/CdSe allowed front side illumination, which no longer has any light absorption loss occurring in back side mode. Furthermore, the nanotubular structure of the TNTs had a much longer electron lifetime than the TNPs due to the fewer recombination centers. These contributed to the significantly improved J_{sc} and V_{oc} values. These results provide insight into the QD-assembled electrodes for various applications, such as solar cells, catalysts and photoelectrochemical cells.

Acknowledgments

This work was supported by Basic Science Research Program through the National Research Foundation of Korea (NRF) funded by the Ministry of Education, Science and Technology (grant number 2012R1A1A4A01009654) and also supported by the Human Resources Development Program of Korea Institute of Energy Technology Evaluation and Planning (KETEP) grant (No. 20104010100580) funded by the Korean Ministry of Knowledge Economy.

References

[1] O'Regan, B., & Grätzel, M., (1991). *Nature*, *353*, 737.
[2] Lee, J. P., Yoo, B., Suresh, T., Kang, M. S., Vital, R., & Kim, K.-J., (2009). *Electrochim. Acta*, *54*, 4365.
[3] Grätzel, M., (2001). *Nature*, *414*, 338.
[4] Park, J.-H., Kim, J.-Y., Kim, J.-H., Choi, C.-J., Kim, H., Sung, Y.-E., & Ahn, K.-S., (2011). *196*, 8904.
[5] Yella, A., Lee, H. W., Tsao, H. N., Yi, C., Chandiran, A. K., Nazeeruddin, M., Diau, E. W.-G., Yeh, C.-Y., Zakeeruddin, S. M., & Grätzel, M., (2011). *334*, 629.
[6] Hodes, G., (2008). *J. Phys. Chem. C*, *112*, 17778.
[7] Chang, C.-H., & Lee, Y.-L., (2007). *Appl. Phys. Lett.*, *91*, 053503.
[8] Lee, W. J., Kang, S.-H., Min, S. K., Sung, Y.-E., & Han, S.-H., (2008). *Electrochem. Commun.*, *10*, 1579.
[9] Shen, Q., Kobayashi, J., Diguna, L. J., & Toyoda, T., (2008). *J. Appl. Phys.*, *103*, 084304.
[10] Lin, S.-C., Lee, Y.-L., Chang, C.-H., Shen, Y.-J., & Yang, Y.-M., (2007). *Appl. Phys. Lett.*, *90*, 143517.
[11] Song, X., Fu, Y.-S., Xie, Y., Song, J.-G., Wang, H.-L., Sun, J., & Du, X.-W., (2010). *Semicond. Sci. Technol.*, *25*, 045031.
[12] Sun, W.-T., Yu, Y., Pan, H.-Y., Gao, X.-F., Chen, Q., & Peng, L.-M. (2008). *J. Am. Chem. Soc.*, *130*, 1124.
[13] Gao, X.-F., Sun, W.-T., Hu, Z.-D., Ai, G., Zhang, Y.-L., Feng, S., Li, F., & Peng, L.-M. (2009). *J. Phys. Chem. C*, *113*, 20481.
[14] Gao, X.-F., H.-B. Li, Sun, W.-T., Chen, Q., Tang, F.-Q., & Peng, L.-M. (2009). *J. Phys. Chem. C*, *113*, 7531.
[15] Archer, M. D., Nozik, A. J., *et al.* (2008). *Nanostructured and photoelectrochemical systems for solar photon conversion*. R. J. D. Miller, R. Memming (Eds.), Chapter 2, p. 130, Imperial College Press: Singapore.
[16] Ahn, K.-S., Kang, M. S., Lee, J. K., Shin, B. C., & Lee, J. W. (2006). *Appl. Phys. Lett.*, *89*, 013103.
[17] Nah, Y.-C., Paramasivam, I., & Schmuki, P. (2010) *ChemPhysChem*, *11*, 2698.
[18] Nacak, J. M., Tsuchiya, H., Taveira, L., Aldabergerova, S., & Schmuki, P. (2005). *Angew. Chem. Int. Ed.*, *44*, 7463.
[19] Kang, S. H., Kim, Y. S., Kim, J.-Y., & Sung, Y.-E. (2009) *Nanotechnol*, *20*, 355307.
[20] Paulose, M., Shankar, K., Varghese, O. K., Mor, G. K., & Grimes, C. A. (2006). *J. Phys. D: Appl. Phys.*, *39*, 2498.
[21] Zhao, L., Yu, J., Fan, J., Zhai, P., & Wang, S. (2009). *Electrochem. Commun.*, *9*, 2052.
[22] Yu, J., Fan, J., & Cheng, B. (2011). *J. Power Sources*, *196*, 7891.
[23] Chen, Q., & Xu, D. (2009). *J. Phys. Chem. C*, *113*, 6310.
[24] Park, J. H., Lee, T.-W., & Kang, M. G. (2008) *Chem. Commun.*, 2867.
[25] Choi, J., Park, S.-H., Kwon, Y. S., Lim, J., Song, I. Y., & Park, T. H. (2012) *Chem. Commun.*, *48*, 8748.
[26] Lei, B.-X., Liao, J.-Y., Zhang, R., Wang, J., Su, C.-Y., & Kuang, D.-B. (2010) *J. Phys. Chem. C*, *114*, 15228.

[27] Guan, X.-F., Huang, S.-Q., Zhang, Q.-X., Shen, X., Sun, H. C., Li, D.-M., Luo, Y.-H., Yu, R.-C., & Meng, Q.-B. (2011). *Nanotechnol, 22*, 465402.
[28] Lee, H.-J., Wang, M., Chen, P., Gamelin, D. R., Zakeeruddin, S. M., Grätzel, M., & Nazeeruddin, M. K. (2009). *Nano Lett.*, *9*, 4221.
[29] Kim, H. S., Jung, S.-W., Ahn, K.-S., & Kang, S. H. (2013) *Current Appl. Phys.*, In press.
[30] Huang, S., Zhang, Q., Huang, X., Guo, X., Deng, M., Li, D., Luo, Y., Shen, Q., Toyoda, T., & Meng, Q. (2010). *Nanotechnol*, *21*, 3752021.
[31] Zaban, A., Greenshtein, M., & Bisquert, J. (2003) *ChemPhysChem*, *4*, 859.
[32] Zhu, K., Neale, N. R., Miedaner, A., & Frank, A. J. (2007). *Nano Lett.*, *7*, 69.
[33] Mor, G. K., Shankar, K., Paulose, M., Varghese, O. K., & Grimes, C. A. (2006). *Nano Lett.*, *6*, 215.
[34] O'Regan, B. C., Durrant, J. R., Sommeling, P. M., & Bakker, N. J. (2007). *J. Phys. Chem. C*, *111*, 14001.
[35] Wang, Z.-S., Yamaguchi, T., Sugihara, H., & Arakawa, H. (2005). *Langmuir*, *21*, 4272.
[36] Nazeeruddin, M. K., Kay, A., Rodicio, I., Humphry-Baker, R., Müller, E., Liska, P., Vlachopoulos, N., & Grätzel, M. (1993). *J. Am. Chem. Soc.*, *115*, 6382.
[37] Ko, Y.-S., Kim, M.-H., & Kwon, Y.-U. (2008). *Bull. Korean Chem. Soc.*, *29*, 463.